# The Calibration and use of CFD Models to Examine Scour from Stormwater Treatment Devices – Hydrodynamic Analysis

H. Avila[1]* and R.Pitt[2]

[1] *Ph.D. Candidate in Civil Engineering – Water Resources Engineering, The Department of Civil, Construction and Environmental Engineering, The University of Alabama, Tuscaloosa, AL 35487 USA*

[2] *Cudworth Professor of Urban Water Systems, The Department of Civil, Construction, and Environmental Engineering, The University of Alabama, Tuscaloosa, AL 35487 USA*

**Corresponding author, e-mail hfavilarangel@bama.ua.edu*

## ABSTRACT

Understanding the hydrodynamics in a stormwater control device is fundamental to evaluate the potential scour of the pre-deposited sediment. Computational Fluid Dynamics - CFD models are useful to achieve this purpose. However, in order to reduce the uncertainty of the computational results, it is necessary to calibrate the parameters that domain the hydrodynamics. Calibration is one of the most important and critical phases when a computational model is used to evaluate different alternatives of design or scenarios. The basic principle of calibration is the estimation of parameters of a numerical model by analytically comparing real data with simulated results under different computational scenarios in order to achieve an acceptable level of similarity. Once the computational model is calibrated and validated with additional experimental data, several new scenarios can be simulated and their results can be accepted with a low level of uncertainty. This paper describes the process, methodology, and results obtained during the calibration of a 3D CFD model evaluating the hydrodynamics in a conventional catchbasin sump prior to the sediment scour analysis. 2D and 3D CFD models and a full-scale physical model were used for this purpose.

## KEYWORDS

Computational Fluid Dynamics (CFD); calibration; hydrodynamics; sediment scour; physical modeling; stormwater treatment device.

## INTRODUCTION

It is a true that CFD numerical analysis is a useful tool to evaluate the hydrodynamics in stormwater treatment devices. However, it is also a fact that the results obtained from numerical analysis contain some level of uncertainty associated with simplifications of the problem, assumption of models and parameters, limitations of the models, among others reasons. This fact becomes more critical when no experimental data is available or no similar simulations have been performed for comparison or validation, especially when several physical phenomena are involved into the analysis, or new sophisticated geometries and designs are proposed.

A conventional catchbasin sump, object of this paper, has a high level of complexity for modeling. An extensive optimization of the mesh resolution in the plunging water jet zone, a variation of turbulent mixing length for the entire control volume, high turbulent flow near the

surface and low turbulent flow near the bottom of the sump, air entrainment, buoyancy, and sediment scour simultaneously all greatly add to the complexity of the model, the computational requirements, and the uncertainty of the numerical results.

Therefore, before preceding with simulations of the sediment scour scenarios and validation of the results with the experimental data, it is fundamental to ensure the correct hydrodynamic behaviour in the control volume, considering all the relevant phenomena and parameters. Obtaining valid numerical results of sediment concentration at the outlet is not enough evidence to believe that the hydrodynamics in the control volume is correct. Especially if the objective is to enhance the hydrodynamic conditions to reduce the sediment scour. For example, a question like, what are the main factors that cause sediment scour: the impacting of the plunging water jet, the secondary flow generated in the control volume, the location of the sediment bed, the geometry of the inlet, etc.?, can be only solved if the hydrodynamics of the flow is well understood.

## METHODOLOGY

Three different analyses have been conducted to achieve a reasonable understanding of the hydrodynamics involved in conventional stormwater catchbasin sumps.

- **2D model:** necessary to have an initial approach to the hydrodynamic of the flow, identify relevant parameters associated with sediment scour, identify capabilities and potential limitations for the 3D numerical analysis, and establish the experimental design for the physical experimentation.
- **Full-scale physical model:** necessary to collect experimental data of the hydrodynamics in the control volume (velocities), the scoured sediment mass, turbidity time series, and particle sizes distribution of the scoured material.
- **3D model:** necessary to understand the hydrodynamics responsible for sediment scour, and simulate several scenarios not performed during the physical experimentation. The 3D model requires prior calibration and validation based on the experimental data obtained from the physical experimentation.

Before the CFD modeling was conducted, a great deal of background work with the model was necessary to ensure reasonable results. CFD modeling is very sensitive to many modeling parameters and options. We based our initial model setup on prior CFD modeling of similar devices as reported in the literature, from discussions with many other CFD modelers, and on prior laboratory and field monitoring results of catchbasins.

### Geometry of the catchbasin sump

The geometry of the catchbasin sump was based on the optimal geometry recommended by Larger, *et al.* (1977), and tested by Pitt (1979, 1985, and 1998). For this geometry, if the outlet diameter is D, the total height of the catchbasin sump is 6.5D and the inside diameter is 4D; the outlet has to be located 4D above the bottom and 2.5D below the top of the catchbasin. The outlet diameter (D) was selected as 300 mm (12 inches). The 2D model was implemented in Fluent 6.2 (ANSYS, 2006) by using the longitudinal center-line cross section on the predominant flow direction, the full-scale physical model was build with a flow capacity of 10 L/s (160 GPM), and the 3D model was implemented in Flow-3D (Flow Science, 2007), (see Figure 1).

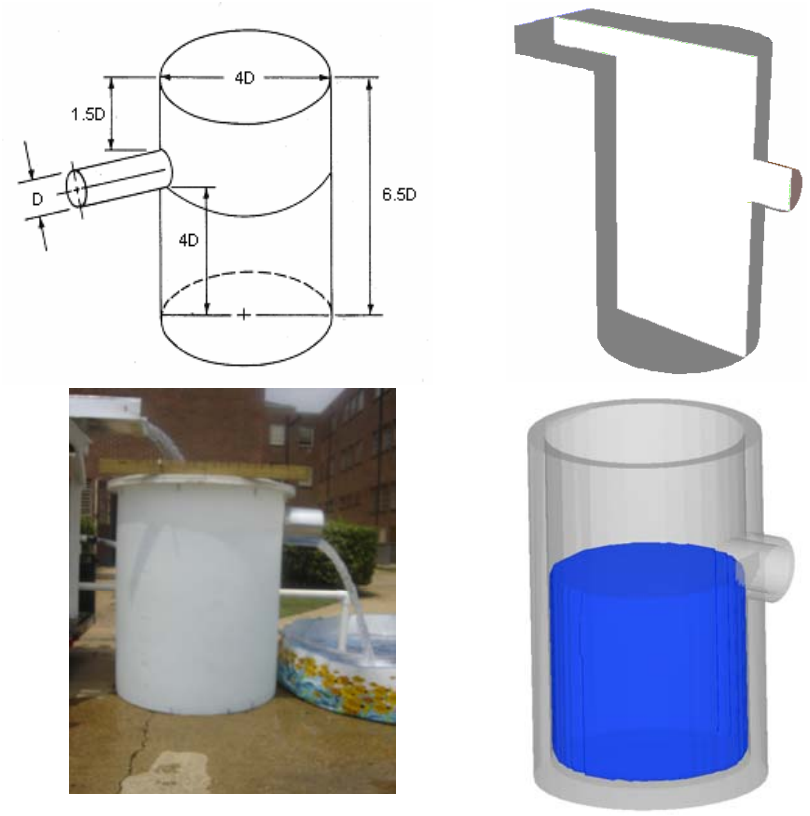


**Figure 1**. Typical catchbasin geometry by Larger, *et al.* (1977) (top left), the 2D CFD longitudinal center-line cross section (top right), the full-scale physical model (bottom left), and the 3D CFD model (bottom right).

**2D Model Evaluation**

Two different sets of modeling experiments were performed to evaluate the factors that affect scour of sediment from stormwater catchbasin sumps: 1) A $2^4$-full factorial experimental design to identify the most significant factors and their interactions considering flow rate, sediment particle size, water depth, and specific gravity; and 2) A response-surface examination of shear stress at different sediment elevations, caused by different flow rates and inlet geometries. Table 1 shows the factors with their corresponding low and high levels.

**Table 1**. Factors and Settings for the $2^4$-full factorial experimental design.

| | Factor | Low Values | High Values |
|---|---|---|---|
| A | Flow rate (L/s) | 1.6 | 20.8 |
| B | Particle size (μm) | 50 | 500 |
| C | Water Depth (m) | 0.2 | 1.0 |
| D | Specific gravity | 1.5 | 2.5 |

For the response-surface examination of shear stress, three different hypothetical location of the sediment bed were evaluated: 1.0, 0.8, and 0.6 m below the outlet. During field monitoring, sediment usually accumulates until it has reached an elevation of about 0.3 m below the outlet (Pitt, 1979 and 1985). Five different flow rates were considered: 2, 5, 10, 20, and 40 L/s; inflowing water was assumed to be relatively clear. These flow rates are within the range used by Metcalf & Eddy *et al.* (1977) in their laboratory studies, and also by the

modeling studies conducted by Faram *et al.* (2003) to evaluate the sediment removal and retention capabilities of stormwater treatment chambers. The scour potential of sediment is indirectly determined by calculating the maximum shear stress on a flat surface (assumed as sediment layer), and comparing it to the permissible shear stress for specific particle sizes. The results response-surface examination of shear stress can be found in Avila *et al.* (2008).

### Full-scale Physical Model

A full-scale physical model was built with a maximum flow capacity of 10 L/s. Two different experimentations were performed:1) A hydrodynamic test, from which velocities in x, y and z directions were measured with an Acoustic Doppler Velocity Meter (ADV) on 155 different locations within the control volume distributed on 5 layers with 31 points each. Three flow rates (2.5, 5.0, and 10 L/s) and two type of inlet geometries were evaluated (50 cm-wide rectangular inlet, and 30 cm circular pipe inlet), and 2) A scour test, from which a turbidity time series, Total Suspended Solids (TSS), and Particle Size Distribution (PSD) were measured at the outlet of the catchbasin. For this test, a sediment mixture was prepared, based on the PSD of pre-deposited sediment found in catchbasins by Valiron and Tabuchi (1992), and Pitt and Khambhammuttu (2006). The sediment mixture was placed on four elevations (10, 25, 46, and 106 cm below the outlet); the scour test was performed with five successive steady flow rates (0.3, 1.2, 3.0, 6.2, and 10.0 L/s) and four impacting tests of 10 L/s each.

### 3D Model Evaluation and Calibration of the Hydrodynamics

The 3D CFD model implemented in Flow-3D represents a conventional catchbasin sump with 50 cm-wide rectangular inlet. The model had the following characteristics: 1) mesh sizes: 230,730 cells, 2) boundary conditions: velocity at the inlet, pressure at the outlet, wall on sides and symmetry on the top, 3) turbulent model: Renormalized group (RNG) model, 4) air entrainment model with buoyancy effect was included, 5) surface tension and wall friction were neglected given the scale characteristics of the flow, 6) time of simulation: 300 sec, 7) the calibration of the model was performed at 10 L/s flow rate, 8) the simulations were performed with a 32-bit system with two 3GB processors in parallel; each simulation file was about 4 GB in size.

## RESULTS AND DISCUSSION

### 2D Model

A multiphase Eulerian model was implemented for the $2^4$-full factorial experimental design. Because the multiphase Eulerian model does not allow an immiscible water-air interphase, the flow was assumed to be a vertical-submersible water jet. As expected, high flows with shallow overlaying water depths (A) result in the fastest washout of the sediment. Particle size alone (B) and particle size and specific gravity combined (BD) had little effect on scour. The presence of the letter represents the corresponding factor at high level and the remaining factors at low level.

An ANOVA with no replicates was used to determine the significance of each factor at 95% confidence level. Significant factors would have a *p*-value equal or smaller than 0.05. The results in Table 2 show that flow rate, particle size, and water depth are significant factors for times greater that 600 sec (10 min). Additionally, the interactions of flow rate-particle size, flow rate-water depth, and particle size-water depth were also significant. However, specific

gravity, or any interaction containing specific gravity, was not significant at the 95% confidence level for any of the evaluated times. These results were used to setup the experimental design with the full-scale physical model.

**Table 2.** ANOVA results: p-values for each treatment at different times.

| | Time (sec) | | | | | |
|---|---|---|---|---|---|---|
| Treatment | 60 | 300 | 600 | 1000 | 1800 | 3000 |
| A | **0.02** | **0.006** | **0.003** | **0.003** | **0.003** | **0.003** |
| B | 0.14 | 0.06 | **0.02** | **0.02** | **0.01** | **0.01** |
| C | **0.02** | **0.01** | **0.009** | **0.009** | **0.01** | **0.008** |
| D | 0.13 | 0.09 | 0.08 | 0.12 | 0.24 | 0.22 |
| AB | 0.15 | 0.08 | **0.03** | **0.03** | **0.04** | **0.06** |
| AC | **0.02** | **0.01** | **0.01** | **0.01** | **0.02** | **0.03** |
| AD | 0.13 | 0.10 | 0.09 | 0.15 | 0.34 | 0.34 |
| BC | 0.17 | 0.17 | 0.10 | 0.07 | 0.05 | **0.04** |
| BD | 0.82 | 0.86 | 0.97 | 0.77 | 0.41 | 0.34 |
| CD | 0.16 | 0.21 | 0.24 | 0.28 | 0.47 | 0.54 |

## Full-scale Physical Model: Experimental Data

Velocity magnitudes and direction, obtained from the hydrodynamic test, showed the effect of the plunging water jet on the control volume. It was possible to identify the velocity pattern at different elevations using different inlet geometries for a range of flow rates between 2.5 and 10 L/s. Figure 2, for example, shows the comparison of mean z-velocities at 36 and 96 cm below the outlet using a 50 cm-rectangular inlet under a 10 L/s flow rate. The figure shows that at 96 cm below the outlet the z-velocities are considerably smaller than the velocities at 36 cm below the outlet. Additionally, it possible to see that there is an important ascending component at 36 cm below the outlet with velocities up to 8.0 cm/s at point 29 which is located close to the outlet.

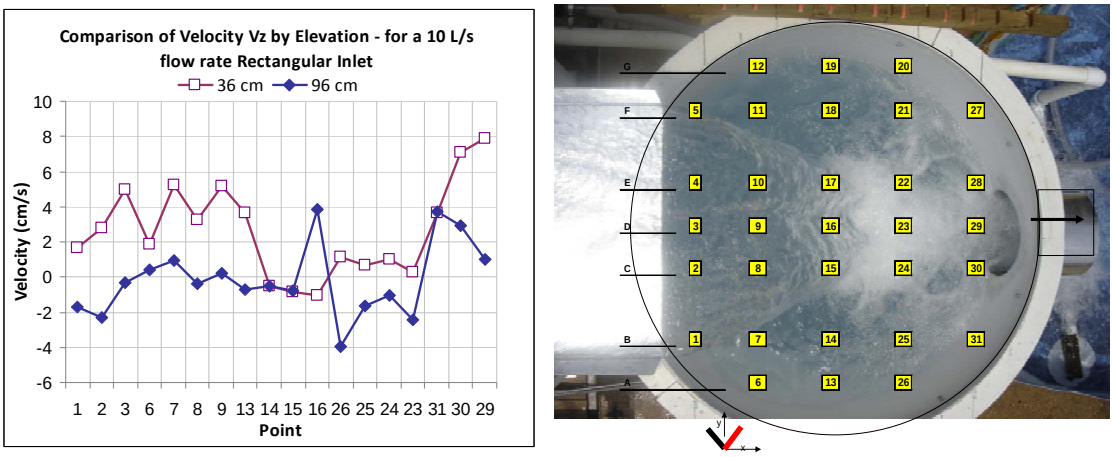


**Figure 2**. Comparison of mean z-velocities on different points located at 36 and 96 cm below the outlet. Test performed with a rectangular inlet and 10 L/s flow rate (left), and Plan view of the catchbasin sump with the location of the measuring points (right).

However, it is also important to consider not only the mean velocity but also its variation. Figure 3 shows the normal probability plot of z-velocities at 36 and 96 cm below the outlet at the point 16 located in the center of the projected top area of the control volume. The figure shows that at 36 cm below the outlet the mean z-velocity is -1.0 cm/s with a standard variation of 3.3 cm/s and at 96 cm below the outlet the z-velocity is 3.8 cm/s with a standard variation of 3.14 cm/s. This shows that, if a control limit of three standard deviations is applied, the velocity magnitudes may be in the same order of magnitude.

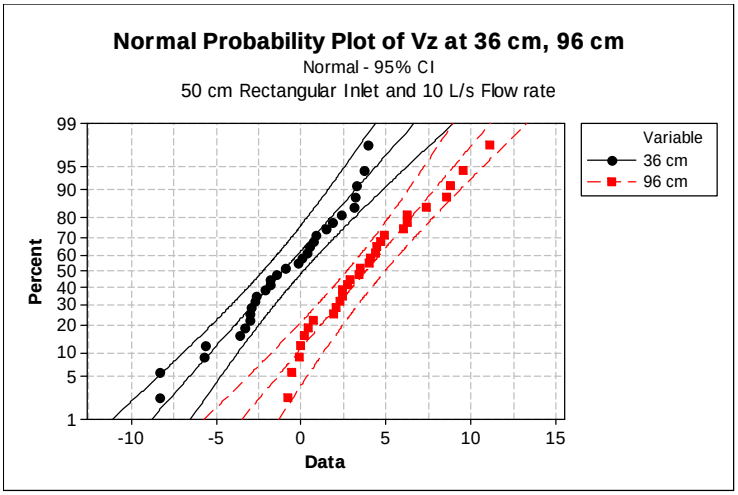


**Figure 3**. Normal probability plots of z-velocities at 36 and 96 cm below the outlet at point 16. These velocities correspond to a scenario with rectangular inlet and 10 L/s flow rate.

The probability plots of the experimental velocities were compared to the simulated data at several points located in the control volume, to evaluate the level of similarity in the mean and standard variation of the velocities.

On the other hand, turbidity time series, Total Suspended Solids (TSS), and scoured particle sizes were measured during the scour test using a pre-deposited sediment particle size distribution with $D_{10}$ = 90 μm, $D_{50}$ = 500 μm, and $D_{90}$ = 2,000 μm. Figure 4 shows the turbidity time series obtained at 10 cm below the outlet (figure on the left) and at 106 cm below the outlet (figure on the right). These figures show that at 10 cm below the outlet it is possible to identify a decreasing exponential pattern under all the series of flow rates tested. The turbidity peak measured at the beginning of each flow rate increases as a function of the flow rate. This pattern will allow one to validate the scour simulations by evaluating the concentration pattern at the outlet under different flow rates. However, no evident pattern was detected when the pre-deposited sediment is located at 106 cm below the outlet.

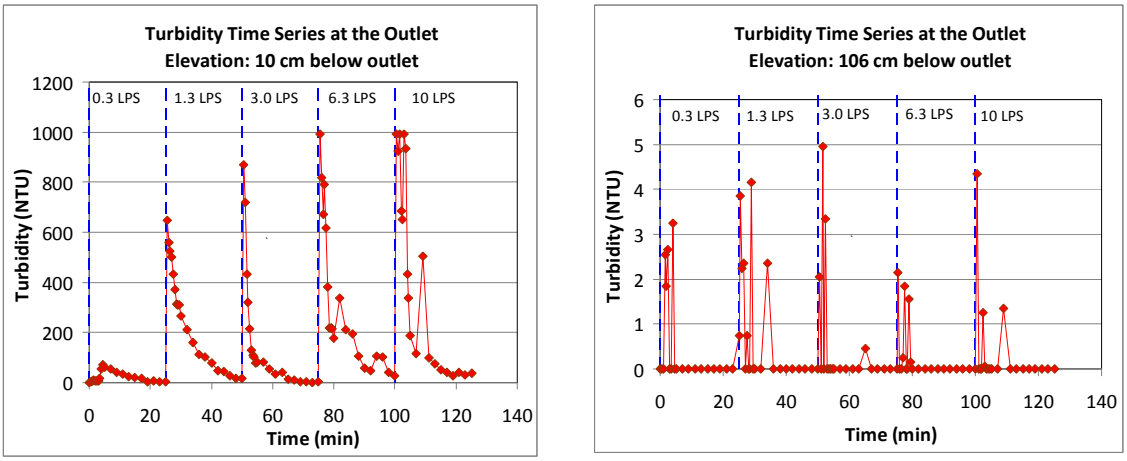


**Figure 4**. Turbidity time series at the outlet for sediment located at 10 cm below the outlet (left) and at 106 cm below the outlet (right).

Additionally, the total scoured sediment mass was determined by measuring the Total Suspended Solids at the outlet considering a composite sample for the first 5 min and another composite sample for the next 20 min. The mass flux rate was determined from these measurements. Figure 5 shows the time series of the cumulative scoured mass for different elevations of sediment below the outlet. These time series will be used for validation of the scour simulations.

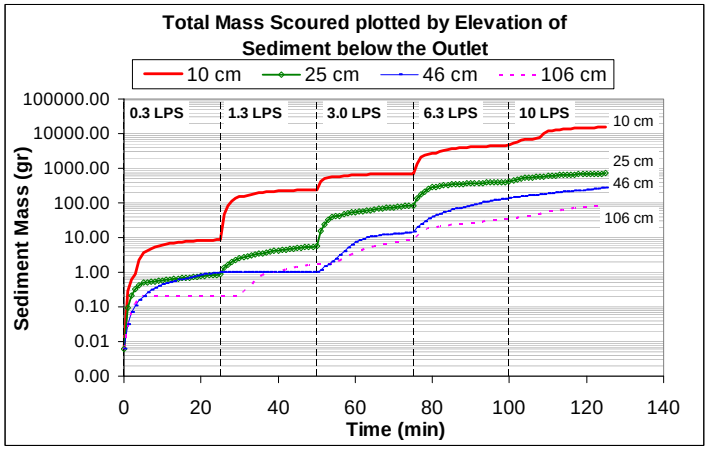


**Figure 5**. Total scoured sediment mass time series by elevation of sediment below the outlet.

### 3D Model: Calibration

The calibration process consisted of the estimation of the relevant parameters of the model to obtain similar simulated and experimental results under a scenario of 10 L/s flow rate. The parameters involved in the calibration were the turbulent mixing length, the air entrainment coefficient, and the air bubble diameter. The calibration was conducted under steady state condition by analytically comparing the simulated and experimental velocities on the points distributed in the control volume. However, considering that the comparison of 155 points for each scenario is a time consuming process, only 25 points located on the center line were selected as a quality control sample. If satisfactory results were obtained for a particular scenario, additional points were evaluated. Further analysis will include the validation of the model using a 5.0 L/s flow rate and the results from the scour test.

An issue of concern on the calibration process is the desired acceptable level of similarity between the simulated and experimental data. Typically, when the data is function of time, the calibration is based on the comparison between a time series of single experimental values and the simulated time series results. However, under steady state conditions, several velocity measurements were taken on a single point, so the comparison of a single value (mean value) is not representative, but the probability distribution of the data in order to consider the range of the velocity magnitudes. The experimental data showed that the velocities under turbulent flow and steady state are normally distributed. Therefore, the complete experimental sample at each point was considered for the calibration.

One of the most time consuming stages during calibration was the creation of the mesh. It is necessary to find a balance between a high mesh resolution for accuracy and a low mesh resolution to reduce the computational time under some particular computer specifications. The resolution of the mesh at the end of the free falling jet for example, needed a very high resolution to capture the thickness of the water jet; however a coarse mesh was applied near the bottom. This process was conducted manually until reaching a reasonable cpu time without significantly sacrificing accuracy. The reduction of cpu time is crucial for calibration, considering that several scenarios need to be tested and each scenarios may take about 24 hours to be completed plus the time for analysis and modifications.

The turbulent mixing length is the characteristic length scale of the energy containing eddies (Flow-3D, 2007). This parameter controls the turbulence energy dissipation. The model uses by default the 7% of the smallest domain dimension. However, this value varies in space and time depending on the characteristics of the flow and geometry of the domain. Therefore, it was necessary to calibrate a value that represents the most significant flow conditions. In this case, the turbulent mixing length was controlled mainly by the impacting zone, where the plunging jet affects the control volume in the catchbasin. A value of turbulent mixing length of 0.5 cm was the optimum calibrated. This parameter was the most sensitive during the calibration.

On the other hand, it was initially expected that the amount of air entrainment due to the plunging water jet was not so high to produce significant buoyancy effect in the flow, and the attenuation of the plunging water jet was mainly due to the impact and turbulent dissipation. However, the physical experimentation showed that amount of air entrainment was high enough to produce density variation and buoyancy in the control volume. Bohrer (1998) evaluated the air entrainment coefficients for developed and undeveloped free falling jets, finding an average estimate of 0.5 for undeveloped free falling jets, corresponding to the evaluated case. The final calibration was achieved using an air entrainment coefficient of 0.5.

The air bubble size under turbulent conditions is inverse function of the turbulent energy dissipation (Hinze, 1955), which is also function of the turbulent kinetic energy. Hence, the greater the turbulent kinetic energy the smaller the air bubble size. However, the model has a limitation of considering only an average bubble size. This calibrated bubble diameter size was 0.1 cm.

Figure 6, shows the 3D simulation of the calibrated model presenting velocity magnitudes (left) and density magnitudes (right). The velocity of the free falling jet impacts the water surface at about 3.0 m/s and the velocity magnitude is reduced down to about 1.0 m/s at only few centimetres below the surface. The turbulent dissipation and the buoyancy effect caused by the air entrainment contribute to this reduction.

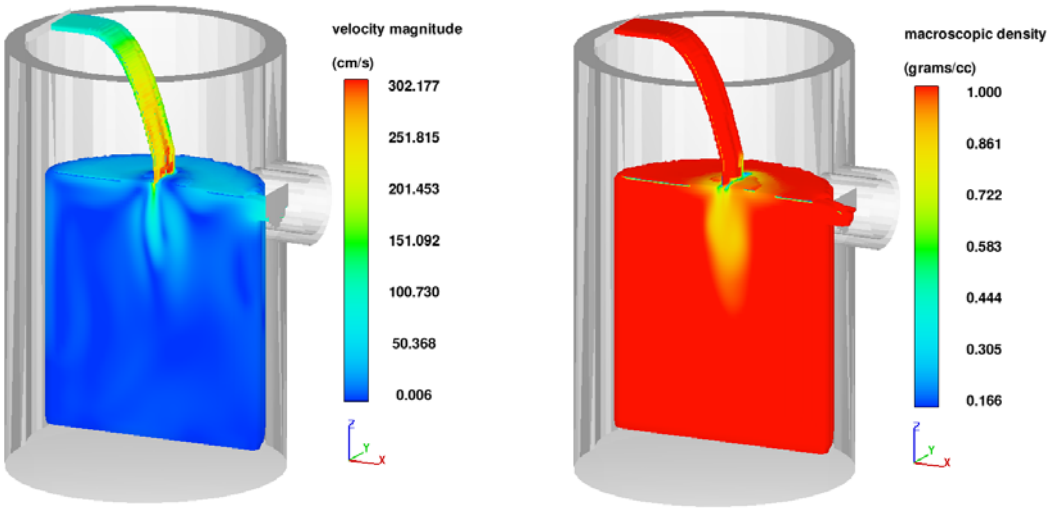


**Figure 6**. Scenario of rectangular inlet with a 10 L/s flow rate. Velocity magnitude in cm/s (left), and macroscopic density in gr/cm$^3$ (right).

The calibration process was based on the comparison of the normal probability plots of simulated and experimental data. Figure 7 shows the comparison between simulated and experimental velocities Vx, Vy, and Vz for 5 points located on the center line at 76 cm below the outlet (out of 155 points in the control volume). The figure shows that the simulated mean velocities are close to the experimental values in all cases. Moreover, the simulated values are also normally distributed. In contrast, it is clear that in some cases the computational model is not capable of reproducing the velocity variation found in the experimental data. However, the slope of the simulated probability plots is typically equal or greater than the experimental, which shows that the simulated velocities fall within the range of the experimental values.

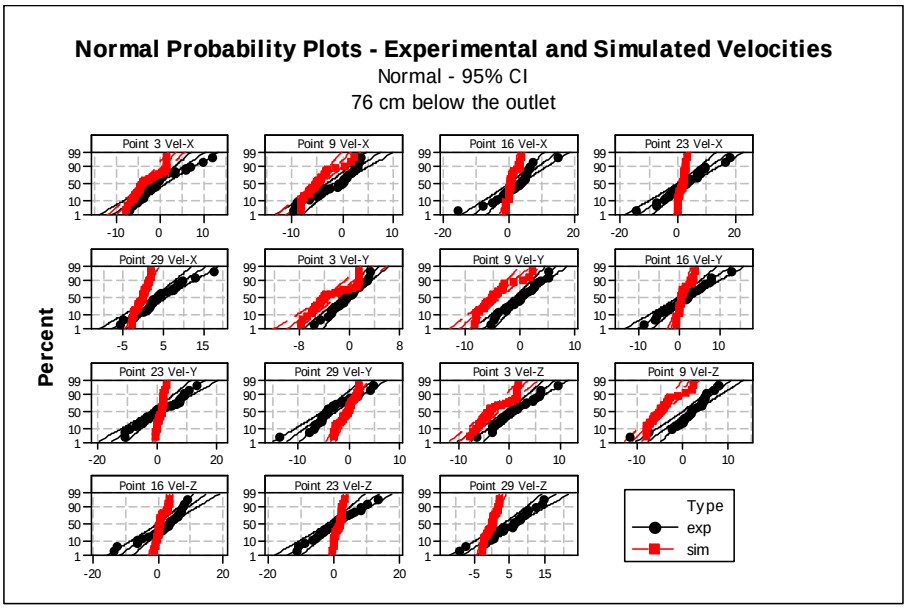


**Figure 7.** Comparison of normal probability plots of simulated and experimental velocities (Vx, Vy, and Vz) on five points located on the center line at 76 cm below the outlet.

## CONCLUSIONS

The main points of this paper are summarized in the following conclusions:

- The calibration of the hydrodynamic parameters of a 3D CFD model prior to the evaluation of the sediment scour in stormwater treatment devices is fundamental when the objective is to understand the causes of scour and enhance the hydrodynamic conditions to reduce the sediment scour.
- The turbulent mixing length was the most sensitive parameter in the calibration. The estimation of this parameter required a good understanding of the hydrodynamics in the control volume. Moreover, the consideration of buoyancy due to air entrainment was also fundamental to represent the hydrodynamic conditions in a conventional catchbasin sump.
- The comparison of normal probability plots of experimental and simulated data is an effective method for calibration which includes not only the mean velocities but also the variation. However, this process may be time consuming when the complexity of the model is high.
- A calibration process requires the evaluation of several hypotheses of parameters, which can take a long time considering that each simulation takes several hours or even days. Therefore, the initial estimation of the parameters is critical to reduce the number of scenarios required for calibration.

## REFERENCES

Avila, H., R. Pitt, and S.R. Durrans. (2008). Factors affecting scour of previously captured sediment from stormwater catchbasin sumps. In: Stormwater and Urban Water Systems Modeling, Monograph 16. (edited by W. James, E.A. McBean, R.E. Pitt and S.J. Wright). CHI. Guelph, Ontario.

Bohrer, J., Abt S., and Wittler R. (1998). Predicting plunge pool velocity decay of free falling rectangular jet. Journal of Hydraulic Engineering, ASCE, Vol. 124, No. 10, pp. 1043-1048. October.

Faram, M.; Harwood, R.; Deahl, P., (2003) "Investigation into the sediment removal and retention capabilities of stormwater treatment chambers," StormCon Conference, Texas, U.S. July.

Flow-3D v.9.2, Flow Science Inc. (2007). User's Manual. www.flow3d.com

Fluent 6.2, ANSYS. (2006). CFD Model User's Manual. http://www.fluent.com

Hinze, J. O., (1955). Fundamentals of the hydrodynamic mechanism of splitting in dispersion processes. Am. Inst. Chem. Eng. J., vol. 1, No. 3, pp. 289-295, September.

Lager, J.A., W.G. Smith, W.G. Lynard, R.M. Finn, and E.J. Finnemore. (1977). Urban stormwater management and technology: Update and Users' Guide. U.S. EPA-600/8-77-014", Cincinnati, U.S. September.

Metcalf & Eddy Inc., Larger J., Smith W., Tchobanoglous G., (1977). Catchbasin technology overview and assessment. U.S. EPA-600/2-77-051, Ohio, U.S.

Pitt, R. (1979). Demonstration of nonpoint pollution abatement through improved street cleaning practices. U.S. EPA. Grant No. S-804432. EPA-600/2-79-161. 270 pages. Cincinnati, U.S. August.

Pitt, R. (1985). Characterizing and controlling urban runoff through street and sewerage cleaning. U.S. EPA. Contract No. R-805929012. EPA/2-85/038. PB 85-186500/AS. Cincinnati, U.S. June.

Pitt, R., Field R. (1998). An evaluation of storm drainage inlet devices for stormawter quality treatment (1998). Proc. Water Environmental Federation Technical Exposition - WEFTEC, Orlando, Florida, U.S.

Pitt, R. and U. Khambhammettu. (2006), "Field verification tests of the UpFlowTM Filter (2006). Small Business Innovative Research, Phase 2 (SBIR2)" U.S. EPA, Edison, NJ, U.S. March.

Valiron F., Tabuchi J.-P. (1992) Maitrise de la pollution urbaine par temps de pluie. étatde l_art. Lavoisier, 564 pgs, ISBN 2-85206-863-X, París.